Clinical Features and Chest CT Manifestations of Coronavirus Disease 2019 (COVID-19) in a Single-Center Study in Shanghai, China

Zenghui Cheng[1]
Yong Lu
Qiqi Cao
Le Qin
Zilai Pan
Fuhua Yan
Wenjie Yang

OBJECTIVE. Confronting the new coronavirus infection known as coronavirus disease 2019 (COVID-19) is challenging and requires excluding patients with suspected COVID-19 who actually have other diseases. The purpose of this study was to assess the clinical features and CT manifestations of COVID-19 by comparing patients with COVID-19 pneumonia with patients with non–COVID-19 pneumonia who presented at a fever observation department in Shanghai, China.

MATERIALS AND METHODS. Patients were retrospectively enrolled in the study from January 19 through February 6, 2020. All patients underwent real-time reverse transcription–polymerase chain reaction (RT-PCR) testing.

RESULTS. Eleven patients had RT-PCR test results that were positive for severe acute respiratory syndrome coronavirus 2, whereas 22 patients had negative results. No statistical difference in clinical features was observed ($p > 0.05$), with the exception of leukocyte and platelet counts ($p < 0.05$). The mean (± SD) interval between onset of symptoms and admission to the fever observation department was 4.40 ± 2.00 and 5.52 ± 4.00 days for patients with positive and negative RT-PCR test results, respectively. The frequency of opacifications in patients with positive results and patients with negative results, respectively, was as follows: ground-glass opacities (GGOs), 100.0% versus 90.9%; mixed GGO, 63.6% versus 72.7%; and consolidation, 54.5% versus 77.3%. In patients with positive RT-PCR results, GGOs were the most commonly observed opacification (seen in 100.0% of patients) and were predominantly located in the peripheral zone (100.0% of patients), compared with patients with negative results (31.8%) ($p = 0.05$). The median number of affected lung lobes and segments was higher in patients with positive RT-PCR results than in those with negative RT-PCR results (five vs 3.5 affected lobes and 15 vs nine affected segments; $p < 0.05$). Although the air bronchogram reticular pattern was more frequently seen in patients with positive results, centrilobular nodules were less frequently seen in patients with positive results.

CONCLUSION. At the point during the COVID-19 outbreak when this study was performed, imaging patterns of multifocal, peripheral, pure GGO, mixed GGO, or consolidation with slight predominance in the lower lung and findings of more extensive GGO than consolidation on chest CT scans obtained during the first week of illness were considered findings highly suspicious of COVID-19.

Keywords: coronavirus disease 2019, COVID-19, CT, pneumonia

doi.org/10.2214/AJR.20.22959

Z. Cheng and Y. Lu contributed equally to this article.

Received February 11, 2020; accepted after revision February 27, 2020.

[1]All authors: Department of Radiology, Ruijin Hospital, Shanghai Jiao Tong University School of Medicine, No. 197, Ruijin Er Rd, Shanghai, 200025, China. Address correspondence to W. Yang (lisa_ywj@163.com).

AJR 2020; 215:1–6

ISSN-L 0361–803X/20/2155–1

A pneumonia of unknown cause that rapidly develops into acute respiratory distress syndrome has been reported since December 2019 in Wuhan, Hubei, China [1–5]. The Chinese Center for Disease Control and Prevention subsequently confirmed that the cause of this pneumonia was a novel coronavirus identified in lower respiratory tract samples. This novel coronavirus has been designated as severe acute respiratory syndrome coronavirus 2 (SARS-CoV-2) by the International Committee on Taxonomy of Viruses. SARS-CoV-2 is a type of RNA virus that belongs to the family of coronaviruses, which primarily leads to respiratory tract infection. Patients infected with SARS-CoV-2 can have severe pneumonia, acute respiratory distress syndrome, and multiple-organ failure develop, which can lead to death. SARS-CoV-2 can be transmitted from human to human through respiratory droplets, contact, and even fecal-oral transmission. Nearly 76,392 cases of coronavirus disease 2019 (COVID-19), the disease caused by SARS-CoV-2, have been confirmed in China, and according to an announcement made by the Chinese government on February

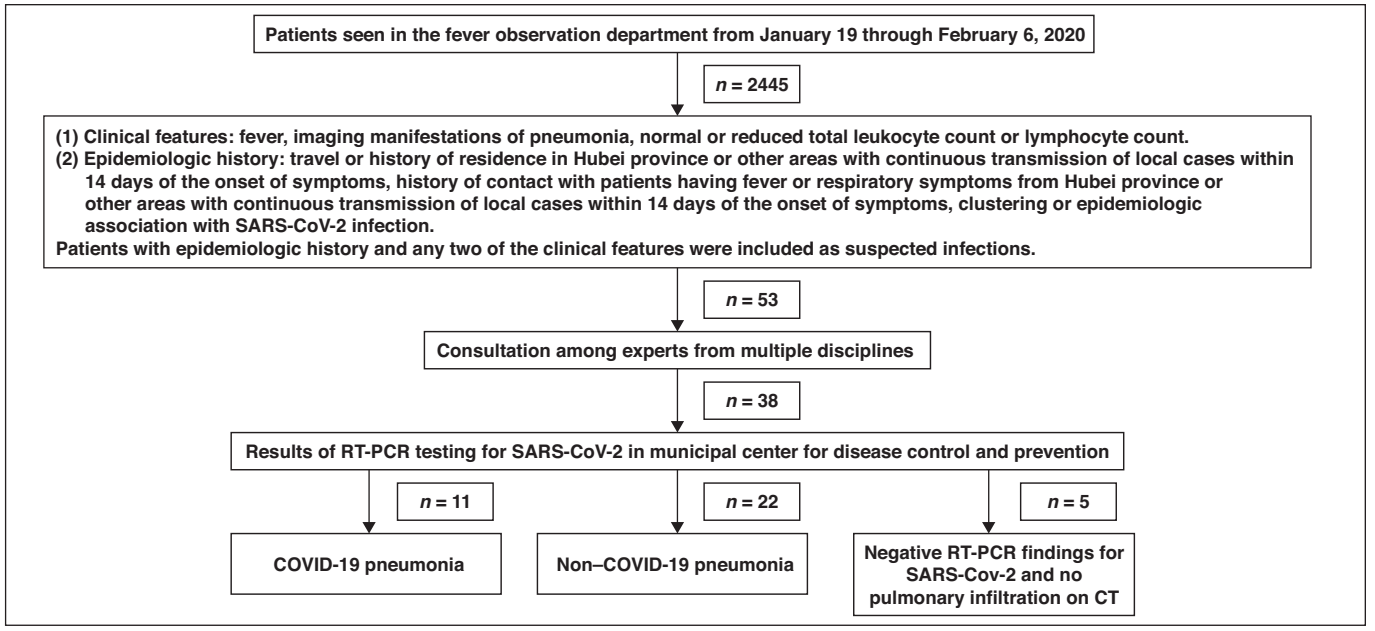

Fig. 1—Flowchart shows details of patient enrollment in study. SARS-CoV-2 = severe acute respiratory syndrome coronavirus 2, RT-PCR = reverse transcription–polymerase chain reaction, COVID-19 = coronavirus disease 2019.

22, 2020, a total of 2348 patients have died. Although prevention and control measures have been applied to prevent further spread of COVID-19 in China, including isolation of people suspected of having the disease, improvement in diagnostic and treatment procedures is still required. Cases of COVID-19 in China are no longer limited to Wuhan, especially after with a large influx of visitors from Wuhan to other cities during the spring festival period, and the disease has quickly spread across China.

Fever observation departments, which are independent emergency departments dedicated to assessing patients with fever or a history of exposure to COVID-19, have rapidly been established nationwide. The goal of these specialized departments is to undertake the diagnosis and evaluation of patients with suspected COVID-19 and to provide frontline diagnosis and confirmation of the disease.

Although preliminary studies [2–5] have reported the clinical features of COVID-19, descriptions of the imaging features of this disease have been limited. Therefore, the purpose of the present study was to identify the clinical features and CT manifestations of COVID-19 and compare them with those of pneumonia occurring in patients with who do not have COVID-19.

Materials and Methods

This retrospective study was approved by institutional review board KY2020–26 at Ruijin Hospital, Shanghai Jiao Tong University School of Medicine, and written informed consent was waived.

Study Participants and Design

Patients were enrolled from January 19 through February 6, 2020, at the fever observation department at our institution, which is dedicated to evaluating patients with fever or a history of exposure to COVID-19. Patients were considered to have suspected COVID-19 and were included in the study if they had two of the following clinical features—fever, manifestations of pneumonia on imaging, and a normal or reduced total leukocyte count or total lymphocyte count—plus an epidemiologic history that included travel or a history of residence in Hubei province or other areas where continuous transmission of local cases occurred within 14 days before onset of symptoms, a history of contact with patients who had fever or respiratory symptoms and were from Hubei province or other areas with continuous transmission of local cases within 14 days before onset of the disease, or clustering or epidemiologic association with the new coronavirus infection [6].

TABLE 1: Baseline Characteristics of Study Population

Characteristic	Patients With COVID-19 (*n* = 11)	Patients With Non–COVID-19 Pneumonia (*n* = 22)	*p*
Age (y), mean ± SD	50.36 ± 15.50	43.59 ± 16.02	0.26
Male sex	8 (72.7)	7 (31.8)	0.06
Exposure	8 (72.7)	7 (31.8)	0.06
Symptom			
Fever	8 (72.7)	17 (77.3)	> 0.99
Cough	7 (63.6)	19 (86.4)	0.19
Sputum	3 (27.3)	11 (50.0)	0.28
Shortness of breath	1 (9.1)	4 (18.2)	0.64
Muscle ache	3 (27.3)	2 (9.1)	0.30
Diarrhea	1 (9.1)	3 (13.6)	> 0.99
Sore throat	1 (9.1)	5 (22.7)	0.64
Interval from symptom onset to admission[a] (d), mean ± SD	4.40 ± 2.00	5.52 ± 4.00	0.41
Peak body temperature (°C), mean ± SD	37.96 ± 0.70	38.15 ± 1.19	0.65

Note—Except where otherwise indicated, data are number (%) of patients. COVID-19 = coronavirus disease 2019.
[a]Admission to fever observation department.

All patients with suspected COVID-19 were assessed by a group of experts from multiple disciplines who determined whether a lower respiratory tract sample should be obtained and should undergo real-time reverse transcription–polymerase chain reaction (RT-PCR) testing. Throat swab specimens were obtained and maintained in a viral transport medium. SARS-CoV-2 was confirmed by a positive RT-PCR test result [1] at the Shanghai Center for Disease Control and Prevention. The RT-PCR test was repeated if the results of the first test were negative. Testing for influenza A virus (swine-origin influenza A [H1N1] virus, influenza A virus subtype H3N2 virus, and avian influenza A [H7N9] virus) and influenza B virus was also performed at our hospital using the RT-PCR assay, as were other routine laboratory tests.

Pneumonia was diagnosed in accordance with the 2007 guidelines of the Infectious Diseases Society of America and the American Thoracic Society [7]. In brief, patients with at least one clinical symptom (i.e., cough, sputum, fever, dyspnea, or pleuritic chest pain), a finding of either coarse crackles on auscultation or elevated inflammatory biomarkers, and observation of a new pulmonary opacification on chest CT were given a diagnosis of pneumonia (Fig. 1). A total of 11 patients with COVID-19 and 22 patients with non–COVID-19 pneumonia were ultimately included in the study.

Clinical Data

All demographic characteristics, clinical signs and symptoms, and laboratory results were retrospectively reviewed.

CT Data

CT data were acquired using a 16-MDCT (LightSpeed Pro16 or LightSpeed VCT; GE Healthcare) or 40-MDCT (uCT 528, Shanghai United Imaging Healthcare) scanner. The imaging parameters used were as follows: tube voltage, 120 kVp; tube current (regulated by automatic dose modulation), 100–350 mA; rotation time, 0.75 second; detector collimation, 40 × 0.55 mm; and table feed, 200 mm per gantry rotation. Primary image reconstruction was performed with a lung kernel at a slice thickness of 1–1.5 mm.

TABLE 2: Comparison of Laboratory Findings Between Patients With Coronavirus Disease 2019 (COVID-19) and Patients With Non–COVID-19 Pneumonia

Laboratory Finding	Patients With COVID-19 (n = 11)	Patients With Non–COVID-19 Pneumonia (n = 22)	p
Leukocyte count (× 10^9 cells/L)	4.38 (3.2–5.01)	5.63 (4.28–7.61)	0.02[a]
Neutrophil count (× 10^9 cells/L)	3.13 (2.02–3.67)	3.49 (2.50–5.71)	0.14
Lymphocyte count (× 10^9 cells/L)	1.10 (1.03–1.33)	1.24 (0.98–1.65)	0.42
Platelet count (× 10^9 cells/L)	143.50 ± 32.63	209.20 ± 57.42	0.00[a]
Hemoglobin level (g/L)	141.00 (133.00–142.00)	136.00 (127.80–143.50)	0.52
C-reactive protein level (mg/L)	14.30 (9.00–27.20)	12.75 (2.53–85.00)	0.77
ESR (mm/h)[b]	70.00 (39.00–77.00)	NA	NA
Transferrin level (g/L)[c]	1.80 (1.64–2.12)	NA	NA

Note—Except where otherwise indicated, data are median (interquartile range). ESR = erythrocyte sedimentation rate, NA = not accessible.
[a]Statistically significant difference.
[b]Normal range, 0.00–15.00 mg/L.
[c]Normal range, 2.00–3.60 g/L.

Imaging Data Analysis

All imaging features were reviewed and evaluated by three experienced radiologists (with 11, 15, and 28 years of experience in thoracic CT), with agreement made via use of a PACS. The CT features included ground-glass opacities (GGO), mixed GGO, consolidation, air bronchogram, nodule, tree-in-bud sign, reticular pattern, subpleural linear opacity, bronchial dilatation, and cystic change. All terms were defined in accordance with Fleischner Society guidelines [8]. The location of the lesion was classified as predominantly central or predominantly peripheral, depending on whether it was found in the inner or outer half of the lung field, respectively. The numbers of affected lung lobes and segments were also counted. Consolidation was classified as subsegmental and segmental, on the basis of its extent. Pleural effusion and mediastinal and hilum lymphadenopathy were also evaluated.

Statistical Analysis

Continuous data with normal and abnormal distribution were expressed as mean (± SD) and median (interquartile range [IQR]) values, respectively, and they were then tested using an unpaired t test and the Wilcoxon rank sum test, respectively. Categoric data were expressed as a count and percentage and were tested using the Fisher exact test. A two-tailed $\alpha < 0.05$ was considered to denote statistical significance. Statistical software (SPSS, version 26.0, SPSS) was used for all analyses.

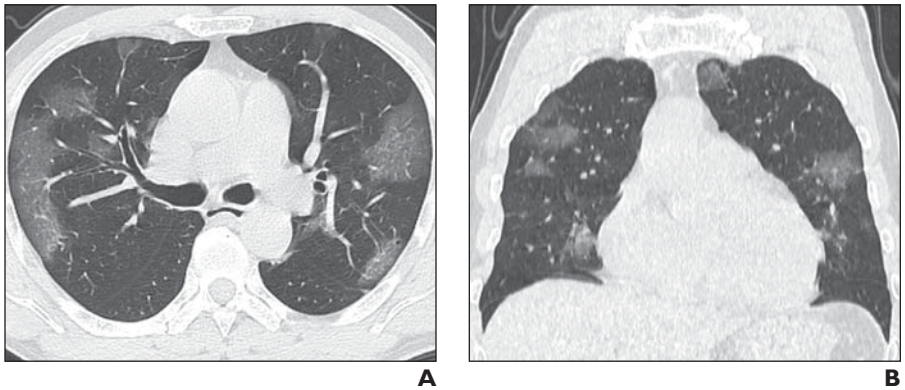

A **B**

Fig. 2—64-year-old man with pneumonia caused by coronavirus disease 2019 who had fever as initial symptom and no history of exposure to coronavirus disease 2019.
A and **B**, Axial unenhanced chest CT image (**A**) and sagittal reconstructed unenhanced chest CT image (**B**) show multifocal, peripheral, patchy ground-glass opacities.

Results

Clinical Findings

Eleven patients had RT-PCR test findings confirmed to be positive for SARS-CoV-2; of these patients, eight patients had a history of exposure to COVID-19. Twenty-two patients with pneumonia had RT-PCR test findings confirmed to be negative for SARS-CoV-2; of these patients, seven had a history of exposure to COVID-19. The mean interval between onset of symptoms and admission to the fever observation department was 4.40 ± 2.00 and 5.52 ± 4.00 days for patients with positive and negative findings, respectively. No statistical difference in clinical features was observed between the two groups except for the leukocyte and platelet counts ($p > 0.05$ for all) (Table 1). The median leukocyte and platelet counts in patients with positive results were lower than those in patients with negative results (leukocyte count, 4.38 vs 5.63 × 10^9 cells/L [$p = 0.02$]; platelet count, 143.5 vs 209.2 × 10^9 cells/L [$p < 0.05$]) (Table 2).

CT Findings

The frequency of opacifications in patients with positive findings and patients with negative findings, respectively, was as follows: GGO, 100.0% (11/11) versus 90.9% (20/22); mixed GGO, 63.6% (7/11) and 72.7% (16/22);

TABLE 3: Comparison of Imaging Features on Chest CT Images of Patients With Coronavirus Disease 2019 (COVID-19) and Patients With Non–COVID-19 Pneumonia

Imaging Feature	Patients With COVID-19 (*n* = 11)	Patients With Non–COVID-19 Pneumonia (*n* = 22)	*p*
Pattern of opacities			
GGO	11 (100.0)	20 (90.9)	0.54
Mixed GGO	7 (63.6)	16 (72.7)	0.70
Consolidation	6 (54.5)	17 (77.3)	0.24
Subsegmental	6 (54.5)	14 (63.6)	
Segmental	0 (0.0)	3 (13.6)	0.53
Air bronchogram	8 (72.7)	6 (27.3)	0.02[a]
Centrilobular nodules	3 (27.3)	17 (77.3)	0.00[a]
Tree-in-bud sign	1 (9.1)	6 (27.3)	0.38
Reticular pattern	9 (81.8)	5 (22.7)	0.00[a]
Subpleural linear opacity	2 (18.2)	6 (27.3)	0.69
Bronchial dilatation	3 (27.3)	3 (13.6)	0.38
Cystic change	1 (9.1)	0 (0.00)	0.33
No. of affected lobes, median (IQR)	5 (4–5)	3.5 (2–4)	0.00[a]
No. of affected segments, median (IQR)	15 (11–17)	9 (2–11)	0.00[a]
Right lower lobe (≥ 4 segments affected)	8 (72.7)	8 (36.4)	0.07
Left lower lobe (≥ 3 segments affected)	7 (63.6)	11 (50.0)	0.71
Primary distribution of opacities			
Central	0 (0.0)	15 (68.2)	
Peripheral	11 (100.0)	7 (31.8)	0.00[a]
Lymphadenopathy	0 (0.0)	3 (13.6)	0.53
Pleural effusion	0 (0.0)	5 (22.7)	0.14

Note—Except where otherwise indicated, data are number (%) of patients. GGO = ground-glass opacity, IQR = interquartile range.
[a]Statistically significant difference.

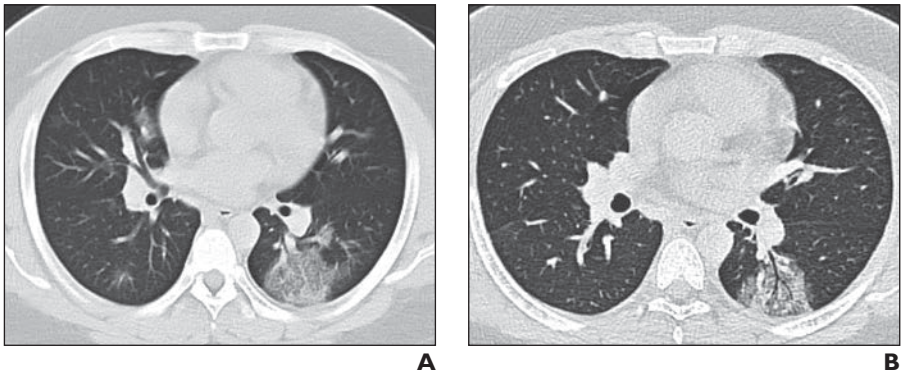

Fig. 3—25-year-old man with pneumonia caused by coronavirus disease 2019 who had fever as initial symptom and no history of exposure to coronavirus disease 2019.
A and **B,** Axial unenhanced chest CT images show multifocal mixed ground-glass opacities with peripheral distribution (**A**), and air bronchogram can be found in left lower lobe ground-glass opacities on thin-section image (**B**).

and consolidation, 54.5% (6/11) and 77.3% (17/22) (Figs. 2–5). The most commonly observed opacification in group A was GGO (100.0% [11/11]). Pulmonary opacifications were predominantly located in the peripheral zone in patients with positive results compared with patients with negative results (100.0% vs 31.8%; $p = 0.00$) (Figs. 2–5). The numbers of involved lung lobes and segments were higher in patients with positive findings than in those with negative findings (five vs 3.5 affected lobes and 15 vs nine affected segments; $p < 0.05$). Although air bronchogram (Fig. 3) and a reticular pattern were seen more frequently in patients with positive results than in patients with negative results (for bronchogram, 72.7% [8/11] vs 27.3% [6/22] [$p = 0.02$]; for reticular pattern, 81.8% [9/11] vs 22.7% [5/22] [$p < 0.05$]), centrilobular nodules (Fig. 6) were less commonly seen (27.3% [3/11] vs 77.3% [17/22]; $p = 0.01$) (Table 3).

Discussion

The fever observation department, an independent emergency department dedicated to patients with fever or a history of exposure to COVID-19, is on the front line of confirming and diagnosing COVID-19. Despite the publication of several preliminary studies of COVID-19, descriptions of the imaging features of this disease have been limited. All preliminary analyses involved patients with confirmed cases of COVID-19. In a study of 41 patients, Huang et al. [2] found that 40 patients (98%) had bilateral involvement. They reported that the typical chest CT findings for patients admitted to the ICU were bilateral, multiple, lobular, and subsegmental areas of consolidation, whereas findings for patients not admitted to the ICU were bilateral GGO and subsegmental areas of consolidation. In a study of 99 patients, Chen et al. [4] reported that 74 patients (75%) had bilateral pneumonia, with just 25 (25%) having unilateral pneumonia. On the other hand, 14 patients (14%) had multiple areas of mottling and GGO. Lei et al. [9] reported a patient with multiple peripheral GGO in both lungs. In a study by Chan et al. [3], six of seven patients had multifocal patchy GGO on CT, especially around the peripheral parts of the lungs. In a study of 51 patients, Song et al. [10] reported that pure GGO were found in 77% of patients and that they showed predominantly bilateral, posterior, and peripheral distribution. To our knowledge, no comparison study of patients who presented in the fever observation department has been performed to date; such a study would be helpful in determining the differential diagnosis for COVID-19.

In the present study, although GGO, mixed GGO, and consolidation were found both in patients with positive RT-PCR test results and in patients with negative RT-PCR test results, the most commonly observed opacification observed in patients with COVID-19 was GGO (100.0% [11/11]), which appeared predominantly in the peripheral zone and most often involved lung lobes and segments. Patients with COVID-19 had a mean interval of 4.40 ± 2.00 days between the onset of symptoms and the first visit to the fever observation department. This strongly suggests that GGO may be the most common imaging manifestation among patients with COVID-19 who are seen in the fever observation department, especially among patients with a history of exposure to COVID-19, which is helpful in diagnosing and isolating cases while they are in the early stage of disease.

It is worth mentioning that in two of the 11 patients who presented with pure GGO or mixed GGO, the appearance of the GGO was round or oval instead of patchy (Fig. 4). Physicians and radiologists on the front line should keep in mind the diversity of imaging presentations of COVID-19. An RT-PCR test remains necessary for patients with uncertain imaging findings and is crucial for control of the outbreak, especially during this early period of the outbreak when the history of exposure may be unknown.

Compatible with findings of a previous study by Chan et al. [3], pleural effusion and lymphadenopathy were not found. Cystic changes and tree-in-bud sign were found in only one of the patients with COVID-19 during their first visit to the hospital, and these findings also were also not found in patients with non–COVID-19 pneumonia, according to previously published studies [11–16].

Consistent with findings of previous studies [2, 4, 5], COVID-19 was more often found in men than in women in our study, having been diagnosed in eight men and three women. A potential explanation for this finding may be protection provided by the X chromosome and sex hormones, which play an important role in innate and adaptive immunity [4].

Chen et al. [4] proposed the MuLBSTA score (the multilobular infiltration, hypolymphocytosis, bacterial coinfection, smoking history, hypertension, and age score) as an early warning model for predicting mortality associated with viral pneumonia in patients receiving treatment for COVID-19. The MuLBSTA scoring system includes the following six indexes: multilobular opacification, lymphopenia, bacterial coinfection, smoking history, hypertension, and age. The youngest patient in the present study, a 25-year-old man (Fig. 3) with a low MuLBSTA score of 5 but with involvement of all

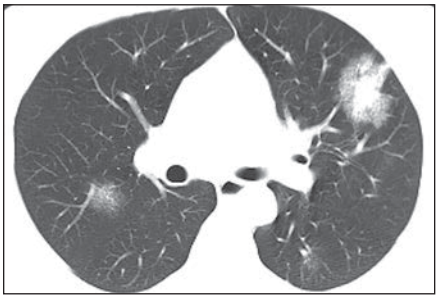

Fig. 4—37-year-old man with pneumonia caused by coronavirus disease 2019 who had fever as initial symptom and history of exposure to coronavirus disease 2019. Unenhanced chest CT image shows multiple, round mixed ground-glass opacities with predominantly peripheral distribution.

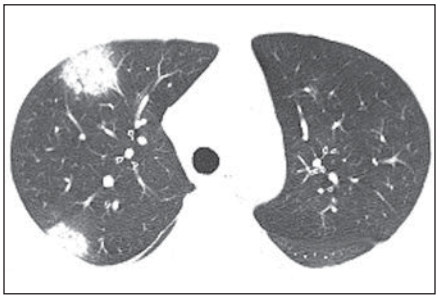

Fig. 5—39-year-old man with pneumonia caused by coronavirus disease 2019 who had fever as initial symptom and history of exposure to coronavirus disease 2019. Unenhanced chest CT image shows subpleural round consolidations in right upper lobe.

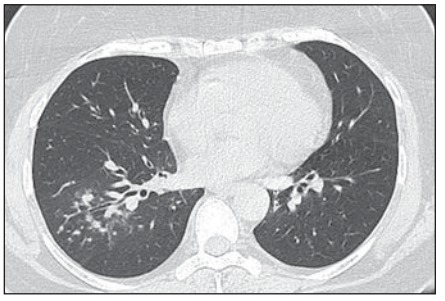

Fig. 6—51-year-old woman with pneumonia not caused by coronavirus disease 2019 who had fever as initial symptom and no history of exposure to coronavirus disease 2019. Unenhanced CT image of chest shows tree-in-bud sign in right lower lobe.

five lung lobes, had rapid disease progression and was treated with extracorporeal membrane oxygenation. A possible explanation for this discrepancy may be that the cytokine storm was associated with disease severity [2] regardless of the clinical background of the patient. Further investigation with use of a bigger sample size is needed to explore the applicability of the MuLBSTA score in predicting the prognosis of COVID-19.

Human coronaviruses are considered important pathogens that cause respiratory infection. Two other coronavirus outbreaks have been reported in the 21st century, including an outbreak of severe acute respiratory syndrome coronavirus in Guangdong province, China, and an outbreak of Middle East respiratory syndrome coronavirus. These two highly pathogenic viruses, severe acute respiratory syndrome coronavirus and Middle East respiratory syndrome coronavirus, generally caused severe respiratory syndrome in humans. In contrast, the severity of COVID-19 has tended to be less severe, although deaths have been reported [2–5]. Although all three of these coronavirus infections have similar common manifestations (i.e., unilateral or bilateral GGO or consolidation) on radiography at presentation, COVID-19 shows more extensive GGO than consolidation, which is consistent with clinical findings [11–16].

There is a wide range of CT manifestations of viral pneumonia. Although not all cases of viral pneumonia have typical imaging patterns, most cases have similar manifestations on imaging and are related to the pathogenesis of pulmonary viral infection. For example, pneumonia caused by varicella-zoster virus shows pulmonary nodulation with a surrounding halo or patchy GGO in both lungs [17]. Moreover, influenza A virus infection presents as multiple areas of consolidation and diffuse GGO, which is similar to the presentation of COVID-19 pneumonia [18, 19]. This may confound confirmation of a cause, especially against a background of the ongoing spread of COVID-19 and the circulation of other respiratory viruses.

The following limitations of the present study should be mentioned. First, the number of cases is small. This is a case series of patients admitted to a fever observation department; a larger cohort study would be helpful to further explore the details of imaging findings. Statistical tests and *p* values should be interpreted with caution because of the small sample size. Second, all imaging findings were collected in the fever observation department, where patients were seen during the early stage of the disease. Because our institution undertakes the diagnosis and investigation of suspected cases of COVID-19, once a patient's diagnosis is confirmed, the patient will be referred to the local center for disease control and prevention. Further studies that include follow-up CT examinations are needed to investigate the entire course of the disease. However, the findings of the present study permit early assessment of the imaging characteristics of COVID-19. Third, the infectious cause of non–COVID-19 pneumonia remains unclear because once COVID-19 infection was excluded, patients with negative findings for COVID-19 were rapidly discharged by the fever observation department. Finally, the only additional testing performed for the patients was testing for the influenza A virus (swine-origin influenza A [H1N1] virus, influenza A virus subtype H3N2 virus, and avian influenza A [H7N9] virus) and the influenza B virus.

Conclusion

During this outbreak of COVID-19, findings considered highly suspicious for the presence of the disease have included an imaging pattern of multifocal, peripheral, pure GGO, mixed GGO, or consolidation, with distribution slightly predominant in the lower lung and with GGO observed more extensively than consolidation on CT scans obtained during the first week of the illness.

Acknowledgment

We thank E. Mark Haacke for his great efforts in revising this article.

References

1. Zhu N, Zhang D, Wang W, et al.; China Novel Coronavirus Investigating and Research Team. A novel coronavirus from patients with pneumonia in China, 2019. *N Engl J Med* 2020; 382:727–733
2. Huang C, Wang Y, Li X, et al. Clinical features of patients infected with 2019 novel coronavirus in Wuhan, China. *Lancet* 2020; 395:497–506
3. Chan JF, Yuan S, Kok KH, et al. A familial cluster of pneumonia associated with the 2019 novel coronavirus indicating person-to-person transmission: a study of a family cluster. *Lancet* 2020; 395:514–523
4. Chen N, Zhou M, Dong X, et al. Epidemiological and clinical characteristics of 99 cases of 2019 novel coronavirus pneumonia in Wuhan, China: a descriptive study. *Lancet* 2020; 395:507–513
5. Li Q, Guan X, Wu P, et al. Early transmission dynamics in Wuhan, China, of novel coronavirus-infected pneumonia. *N Engl J Med* 2020 Jan 29 [Epub ahead of print]
6. National Health Commission of the People's Republic of China website. Strategy of diagnosis and treatment of 2019 novel coronavirus pneumonia, 4th version. www.nhc.gov.cn/yzygj/s7653p/202001/4294563ed35b43209b31739bd0785e67/files/7a9309111267475a99d4306962c8bf78.pdf. Accessed March 10, 2020
7. Mandell LA, Wunderink RG, Anzueto A, et al.; Infectious Diseases Society of America; American Thoracic Society. Infectious Diseases Society of America/American Thoracic Society consensus guidelines on the management of community-acquired pneumonia in adults. *Clin Infect Dis* 2007; 44(Suppl 2):S27–S72
8. Hansell DM, Bankier AA, MacMahon H, McLoud TC, Müller NL, Remy J. Fleischner Society: glossary of terms for thoracic imaging. *Radiology* 2008; 246:697–722
9. Lei J, Li J, Li X, Qi X. CT imaging of the 2019 novel coronavirus (2019-nCoV) pneumonia. *Radiology* 2020 Jan 31 [Epub ahead of print]
10. Song F, Shi N, Shan F, et al. Emerging coronavirus 2019-nCoV pneumonia. *Radiology* 2020 Feb 6 [Epub ahead of print]
11. Müller NL, Ooi GC, Khong PL, Nicolaou S. Severe acute respiratory syndrome: radiographic and CT findings. *AJR* 2003; 181:3–8
12. Müller NL, Ooi GC, Khong PL, Zhou LJ, Tsang KW, Nicolaou S. High-resolution CT findings of severe acute respiratory syndrome at presentation and after admission. *AJR* 2004; 182:39–44
13. Chan MS, Chan IY, Fung KH, Poon E, Yam LY, Lau KY. High-resolution CT findings in patients with severe acute respiratory syndrome: a pattern-based approach. *AJR* 2004; 182:49–56
14. Wong KT, Antonio GE, Hui DS, et al. Thin-section CT of severe acute respiratory syndrome: evaluation of 73 patients exposed to or with the disease. *Radiology* 2003; 228:395–400
15. Ajlan AM, Ahyad RA, Jamjoom LG, Alharthy A, Madani TA. Middle East respiratory syndrome coronavirus (MERS-CoV) infection: chest CT findings. *AJR* 2014; 203:782–787
16. Das KM, Lee EY, Langer RD, Larsson SG. Middle East respiratory syndrome coronavirus: what does a radiologist need to know? *AJR* 2016; 206:1193–1201
17. Koo HJ, Lim S, Choe J, Choi SH, Sung H, Do KH. Radiographic and CT features of viral pneumonia. *RadioGraphics* 2018; 38:719–739
18. Lee JE, Choe KW, Lee SW. Clinical and radiological characteristics of 2009 H1N1 influenza associated pneumonia in young male adults. *Yonsei Med J* 2013; 54:927–934
19. Wang Q, Zhang Z, Shi Y, Jiang Y. Emerging H7N9 influenza A (novel reassortant avian-origin) pneumonia: radiologic findings. *Radiology* 2013; 268:882–889